Nonlinear Network Description for Many-Body Quantum Systems in Continuous Space

Michele Ruggeri,[1] Saverio Moroni,[2] and Markus Holzmann[3,4]
[1]Max Planck Institute for Solid State Research, Heisenbergstr. 1, 70569 Stuttgart, Germany
[2]DEMOCRITOS National Simulation Center, Istituto Officina dei Materiali del CNR and SISSA, Via Bonomea 265, I-34136 Trieste, Italy
[3]Univ. Grenoble Alpes, CNRS, LPMMC, 3800 Grenoble, France
[4]Institut Laue Langevin, BP 156, F-38042 Grenoble Cedex 9, France

(Received 8 November 2017; published 17 May 2018)

We show that the recently introduced iterative backflow wave function can be interpreted as a general neural network in continuum space with nonlinear functions in the hidden units. Using this wave function in variational Monte Carlo simulations of liquid ^{4}He in two and three dimensions, we typically find a tenfold increase in accuracy over currently used wave functions. Furthermore, subsequent stages of the iteration procedure define a set of increasingly good wave functions, each with its own variational energy and variance of the local energy: extrapolation to zero variance gives energies in close agreement with the exact values. For two dimensional ^{4}He, we also show that the iterative backflow wave function can describe both the liquid and the solid phase with the same functional form—a feature shared with the shadow wave function, but now joined by much higher accuracy. We also achieve significant progress for liquid ^{3}He in three dimensions, improving previous variational and fixed-node energies.

DOI: 10.1103/PhysRevLett.120.205302

Explicit forms of many-body ground state wave functions have played an important role in the qualitative and quantitative understanding of many-body quantum systems. Whereas pairing functions based on Bogoliubov's theory [1] have provided a good description of superfluidity and superconductivity of dilute gases, a full pair-product (Jastrow) wave function is usually the starting point for a microscopic description of liquid helium, the prototype of a strongly interacting, correlated quantum system. Starting from the first variational Monte Carlo (VMC) calculations of McMillan [2], liquid and solid helium—bosonic ^{4}He as well as fermionic ^{3}He—have triggered and challenged microscopic simulations.

For systems described on a lattice, approaches based on matrix product and tensor network states [3–7] have provided an essentially exact description of many generic low dimensional systems. Very recently, neural network states have been shown to lead to excellent results in one and two dimensional lattice models [8–11]. However, generalization of these states to continuous systems [12] in two and three dimensions is difficult or still lacking.

In this Letter we elaborate on a recently introduced [13] class of wave functions in continuous space that includes sets of auxiliary coordinates obtained with iterated backflow transformations. Originally introduced from the perspective of Fermi liquid theory to improve the ground state energy of liquid ^{3}He in two dimension, the underlying structure is shown here to be more general, reflecting the evolution in imaginary time, and leading to an accurate description of a broad class of quantum liquids and solids. The wave function is now viewed as a neural network where the hidden units of layer M are obtained iteratively as a function of the coordinates in layer $M-1$, with layer $M=0$ corresponding to the physical particles. In contrast to neural networks on a lattice, all the functions involved here are in general nonlinear. The network parameters describing the various functions are optimized within VMC simulations.

We apply our description to liquid-solid ^{4}He and liquid ^{3}He, where we obtain a systematic lowering of the energy as we increase the number of layers. For the bosonic systems we benchmark the quality with exact results obtained by stochastic projection Monte Carlo methods. We further show that our wave function is able to describe equally well the fluid and the solid phase with the same functional form, symmetric and translationally invariant.

Since the effective interaction between two helium atoms, $v(r)$, is quantitatively well known, computations can be rather directly compared to experiments. During the years several types of wave functions have been used to simulate ^{4}He. In the first VMC simulations [2], the wave function took into account just two-body interparticle correlations; these wave functions were then generalized to include three-body and higher correlations, $\Psi_T(\mathbf{R}) \propto \exp[-U(\mathbf{R})]$, where $U(\mathbf{R})$ denotes a general, symmetric correlation function, and $\mathbf{R} \equiv (\mathbf{r}_1, \mathbf{r}_2, \ldots, \mathbf{r}_N)$ denotes the coordinate vector of the particles [14,15].

Exact results for bosonic ^{4}He can be obtained improving stochastically the wave function with projector Monte Carlo techniques such as diffusion Monte Carlo (DMC) [16] or

variational path integral methods [17–19]. Starting from any trial wave function, $\Psi_T(\mathbf{R})$, its propagation in imaginary time, τ, can be written as

$$\Psi_\tau(\mathbf{R}) \propto \int d\mathbf{R}' G(\mathbf{R},\mathbf{R}';\tau)\Psi_T(\mathbf{R}'). \quad (1)$$

For small τ, the functional form of G is given by

$$G(\mathbf{R},\mathbf{R}';\tau) \propto \exp\left[-\lambda(\mathbf{R}-\mathbf{R}')^2 - V(\mathbf{R})\right] \quad (2)$$

where $\lambda = m/2\hbar^2\tau$ and $V(\mathbf{R})$ is given by the interparticle potential, $V(\mathbf{R}) = \tau\sum_{i<j} v(r_{ij})$. Large projection times can be reached by iterative application of the short time propagator; the integrals can then be sampled numerically via projection Monte Carlo calculations.

Alternatively, we can consider Eqs. (1) and (2) as an improved variational ansatz for our ground state, the shadow wave function (SWF) [20], and minimize the energy with respect to variations in λ, V, and U. In contrast to the explicit trial wave functions, Ψ_T, used in previous VMC calculations, SWFs are able to describe the melting from solid to liquid ^{4}He without modification of their structure.

Shadow and projector Monte Carlo methods explicitly depend on auxiliary (or hidden) variables, $\mathbf{R}'$. The resulting wave function thus forms a network where the hidden variables are connected to the input layer, $\mathbf{R}$. However, in contrast to many neural network systems on a lattice, the variables inside each layer are connected to each other via the many-body potentials, $V(\cdot)$ and $U(\cdot)$ [see Fig. 1(a)].

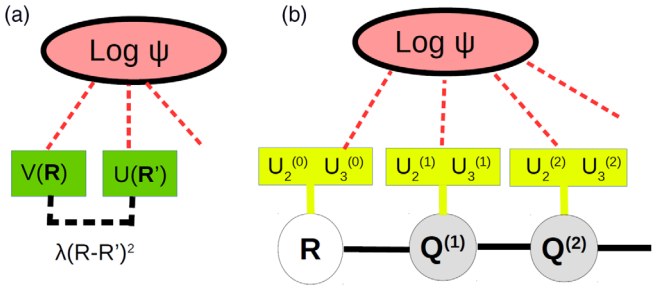

FIG. 1. (a) Schematic representation of a SWF as a nonlinear network. The input layer is formed by the coordinates of the wave function, $\mathbf{R}$, and we have to integrate over the coordinates in the hidden layer, $\mathbf{R}'$. Input and hidden layer coordinates are connected via a Gaussian, whereas the coordinates inside each layer are connected by the many-body correlation potentials, $V(\mathbf{R})$ and $U(\mathbf{R}')$. Including several hidden layers correspond to the application over several projection steps. (b) Structure of the iterated backflow wave function obtained after approximated integration over the hidden layers of SWF and projector Monte Carlo wave functions. Each layer introduces a new set of nonlinear functions $U^{(n)}$ (here, two- and three-body Jastrow forms, $U_2^{(n)}$, $U_3^{(n)}$) and backflow coordinates $\mathbf{Q}^{(n)}$ which depend only on the coordinates of the previous layers $\mathbf{Q}^{(m<n)}$.

Within SWF and projection Monte Carlo calculations, the integration over the variables in the hidden layers is done stochastically which in general leads to a sign (phase) problem whenever G or Ψ_T carries a sign (phase) as for fermionic or time-dependent problems [21–23]. Analytical integration over the hidden layer then becomes extremely important, since the evaluation of the resulting explicit form may be possible within standard VMC without a sign problem.

Since the integration over the hidden variables cannot be done analytically in our case, we approximately perform the integrations in Eq. (1) expanding $U(\mathbf{R}')$ around some positions $\mathbf{Q}$, which will be fixed later. For large λ, we can truncate the expansion after the linear term

$$\Psi_\tau(\mathbf{R}) \approx \int d\mathbf{R}' \exp\left[-\lambda(\mathbf{R}'-\mathbf{R}+\nabla U/2\lambda)^2 - V(\mathbf{R})\right] \times \exp\left[-U-(\mathbf{R}-\mathbf{Q})\cdot\nabla U + (\nabla U)^2/4\lambda\right] \quad (3)$$

where U and ∇U are evaluated at $\mathbf{Q}$, implicitly defined by

$$\mathbf{Q} = \mathbf{R} - \nabla U(\mathbf{Q})/2\lambda. \quad (4)$$

Performing the Gaussian integration, we get

$$\Psi_\tau(\mathbf{R}) \sim \exp\left[-V(\mathbf{R}) - U(\mathbf{Q}) - [\nabla U(\mathbf{Q})]^2/4\lambda\right]. \quad (5)$$

The resulting wave function can then be put into the form

$$\Psi_\tau(\mathbf{R}) = \Phi^{(0)}(\mathbf{R})\cdot\Phi^{(1)}(\mathbf{Q}) \quad (6)$$

where $\Phi^{(n)}(\cdot) = \exp[-U^{(n)}(\cdot)]$ is a correlated wave function containing generalized many-body Jastrow potentials, $U^{(n)}(\cdot)$. Although our derivation suggests explicit expressions for $U^{(n)}$ and $\mathbf{Q}$ in terms of V, U, and λ, we rather retain only the functional form, and simplify Eq. (4) by replacing $\mathbf{Q}$ with $\mathbf{R}$ in the right-hand side. The corresponding parameters are then optimized, such that the wave function, Eq. (6), minimizes some target function, usually taken as the energy or the variance of the local energy [24].

We can further improve our wave function by iteratively applying the propagator to Ψ_τ which approximately leads to a rather simple, iterative structure

$$\Psi^{(M)}(\mathbf{R}) = \prod_{n=0}^{M} \Phi^{(n)}(\mathbf{Q}^{(n)}) \quad (7)$$

where M is the number of iterative backflow transformation. At each level, n, new backflow coordinates are introduced

$$\mathbf{Q}^{(n)} = \mathbf{Q}^{(n-1)} + \nabla U^{(n-1)}(\mathbf{Q}^{(n-1)}) \quad (8)$$

which are built from the backflow and Jastrow potentials of the previous level, $\mathbf{Q}^{(n-1)}$ and $U^{(n-1)}$, respectively, starting from $\mathbf{Q}^{(0)} \equiv \mathbf{R}$. For our explicit calculations, we have used the simplest possible two- and three-body forms in all the generalized Jastrow factors $U^{(n)} \equiv -\log \Phi^{(n)}$ which are parametrized and optimized independently on each level, n.

The approximate integration of the hidden layer structure of SWF and projector Monte Carlo wave function can again be considered as a nonlinear network, represented in Fig. 1(b).

Based on hydrodynamic considerations, backflow has been originally introduced to improve the excitation spectrum of superfluid ^{4}He [27,28], but its importance has soon been recognized for fermionic systems [29] where backflow wave functions reduce the fixed-node error in a broad class of systems. Our heuristic derivation above suggests that the network based on iterative backflow transformations should rather be considered as a generic description for quantum systems in continuous space. However, one may ask if the network can be simplified or made more efficient using a formulation closer to a restricted Boltzmann machine recently applied to discrete lattice systems [8,11].

In order to benchmark the performance of the network, we first focus on a system of N ^{4}He atoms in a cubic simulation box with periodic boundary conditions. The Hamiltonian for this system is given by

$$H = \sum_i \frac{p_i^2}{2m} + \sum_{i<j} v(r_{ij}) \tag{9}$$

with the HFDHE2 potential [30] for $v(r)$.

In the network used to describe the ground state of bosonic ^{4}He, each layer n contains two- and three-body correlations in the generalized Jastrow form

$$\Phi^{(n)}(\mathbf{X}) = e^{-(U_2^{(n)}(\mathbf{X}) + U_3^{(n)}(\mathbf{X}))} \tag{10}$$

with

$$\begin{aligned} U_2^{(n)}(\mathbf{X}) &= \sum_{i<j} u_2^{(n)}(x_{ij}), \\ U_3^{(n)}(\mathbf{X}) &= \sum_i \mathbf{G}_i^{(n)}(\mathbf{X}) \cdot \mathbf{G}_i^{(n)}(\mathbf{X}), \\ \mathbf{G}_i^{(n)}(\mathbf{X}) &= \sum_j (\mathbf{x}_i - \mathbf{x}_j) \zeta^{(n)}(x_{ij}), \end{aligned} \tag{11}$$

characterized by one-dimensional functions, $u_2^{(n)}(x)$ and $\zeta^{(n)}(x)$. Here, the coordinates $\mathbf{X}$ refer to either the bare atomic coordinates ($\mathbf{R} \equiv \mathbf{Q}^{(0)}$) or the transformed ones ($\mathbf{Q}^{(n)}$, $n \geq 1$) which are obtained via

$$\mathbf{q}_i^{(n)} = \mathbf{q}_i^{(n-1)} + \sum_j (\mathbf{q}_i^{(n-1)} - \mathbf{q}_j^{(n-1)}) \eta^{(n)}(q_{ij}^{(n-1)}). \tag{12}$$

The representations of the one-dimensional functions, $u_2^{(n)}$, $\zeta^{(n)}$, and $\eta^{(n)}$, establish the network parameters determined by energy minimization using the stochastic reconfiguration method [31].

Although each hidden layer increases the number of variational parameters, the scaling of the computational effort for evaluation of the wave function with respect to the number of atoms, N, does not increase [13].

In Fig. 2 and Table I, we show the error in the ground state energy obtained for $N = 64$ ^{4}He atoms in three dimensions at equilibrium density ($\rho = 0.0218$ Å^{-3}), close to freezing ($\rho = 0.0262$ Å^{-3}), and for negative pressure ($\rho = 0.0196$ Å^{-3}). The error of the Jastrow or Shadow [32] wave functions ranges in the tenths of K, already reduced significantly by the first backflow layer. Additional layers of backflow transformations bring the error down to a few hundredth K. Zero-variance extrapolation of the energy with a leading linear term [13,24] further approaches the exact ground state energy, the largest error being −0.02 K at the highest density.

A roughly tenfold increase in accuracy is also obtained in the pair correlation function $g(r)$; see Fig. 3.

In order to describe freezing, the liquid and the solid phases are typically described by different functional forms within VMC, as the usual Jastrow wave function is in general unable to localize the atoms in a crystal. This bias propagates even to projector Monte Carlo methods (DMC) based on importance sampling and is only fully eliminated using path integral methods [17,19,33,34]. In order to correctly describe the solid phase within DMC, one usually uses an unsymmetrized Nosanow wave function [35] where the atoms are individually tied to predetermined lattice sites by a one-body term. In this setup, the Jastrow (Nosanow) wave function describes a

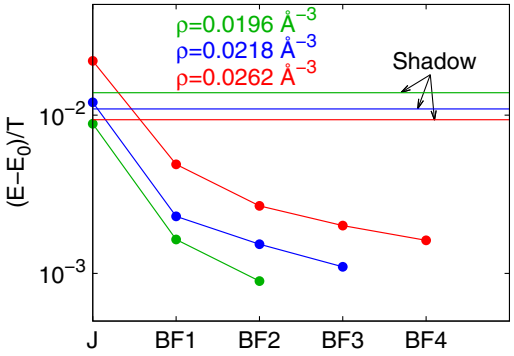

FIG. 2. Difference between the variational energy and the exact value in units of the kinetic energy T for increasing number of hidden layers M of our nonlinear network function for liquid ^{4}He in three dimensions starting from a Jastrow wave function (J) with two- and three-particle correlations, $M = 0$.

TABLE I. Ground-state energy per particle E_{VMC}/N, in K, of liquid ^{4}He in three dimensions at different densities, obtained with VMC using different trial wave functions: Jastrow wave function without backflow (J), and with n iterated backflow transformations (BFn). Variational results obtained with shadow wave functions [32] (E_{SWF}/N) and exact DMC results (E_{DMC}/N) are also shown for comparison. We also report the variance $\sigma^2 = \langle (H - E_{\mathrm{VMC}})^2 \rangle$ of E_{VMC} and the extrapolation of E_{VMC}/N to zero variance [13].

	$\rho = 0.0196$ Å^{-3}			
	E_{VMC}/N	σ^2/N	E_{SWF}/N	E_{DMC}/N
J	−6.8593(10)	14.80	−6.765(8)	−7.0243(6)
BF1	−6.9936(14)	3.03		
BF2	−7.0076(15)	2.14		
Extrap.	−7.033(2)			
	$\rho = 0.0218$ Å^{-3}			
	E_{VMC}/N	σ^2/N	E_{SWF}/N	E_{DMC}/N
J	−6.9137(10)	21.40	−6.937(6)	−7.1691(12)
BF1	−7.1204(12)	5.22		
BF2	−7.1367(10)	3.30		
BF3	−7.1458(14)	2.36		
Extrap.	−7.169(3)			
	$\rho = 0.0262$ Å^{-3}			
	E_{VMC}/N	σ^2/N	E_{SWF}/N	E_{DMC}/N
J	−6.0220(20)	49.99	−6.350(6)	−6.5921(20)
BF1	−6.4656(25)	11.20		
BF2	−6.5230(17)	9.34		
BF3	−6.5402(13)	5.84		
BF4	−6.5502(14)	6.87		
Extrap.	−6.615(2)			

metastable liquid (solid) phase at densities higher (lower) than the coexistence region.

One important conceptual progress of SWF was the possibility to describe both liquid and solid ^{4}He within the same wave function [20], without explicitly breaking translational invariance or Bose symmetry. Remarkably, this feature is shared by our network wave function. In Fig. 4, we show the performance of the network wave functions for $N = 16$ ^{4}He atoms in two dimensions around the liquid-solid transition [36]. Again, our backflow network function achieves a roughly tenfold reduction of the variational error with respect to Shadow [37], Jastrow, and Nosanow wave functions—over a large density range and across a phase transition [38]. For the higher density, $\rho = 0.09$ Å^{-2}, the pair distribution function $g(x, y)$ is hardly distinguishable from the Nosanow (bona fide solid) result. For the lowest density $g(x, y)$ turns into a radial, liquidlike pair distribution function, while at coexistence it is intermediate between the Nosanow and Jastrow results, much closer to the former [24].

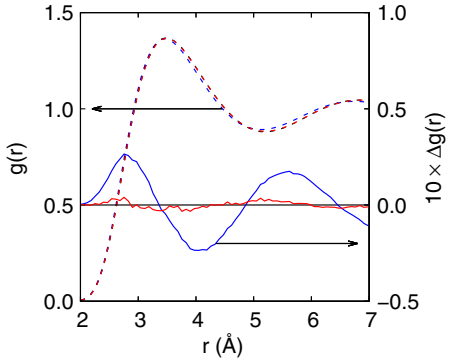

FIG. 3. Pair correlation functions $g(r)$ for liquid ^{4}He in three dimensions at equilibrium density. Dashed lines (left scale) show variational results without backflow terms (blue) and with three backflow iterations (red), as well as DMC results (black, barely visible behind the red dashes; extrapolated estimate [16] using the BF3 trial wave function). Solid lines (right scale) show a tenfold magnification of the deviation between the VMC and DMC results.

Up to now, we have demonstrated the quality of our backflow network to describe bosonic quantum systems, where stochastic projection Monte Carlo methods provide exact results for benchmarking. Now, we show that our approach significantly improves the description of strongly correlated fermions in three dimensions, similar to previous results [13] obtained for two dimensional liquid ^{3}He. In Table II we list estimates of the ground-state energy obtained with different wave functions for $N = 66$ ^{3}He atoms in three dimensions, at equilibrium and freezing density. The previous best estimates [15] were obtained introducing explicit correlations up to four particles in the Jastrow factor and three particles in the backflow coordinates. The results from Ref. [15] included in Table II refer to a spin-singlet pairing wave function, which performs marginally better than a Slater determinant of plane waves.

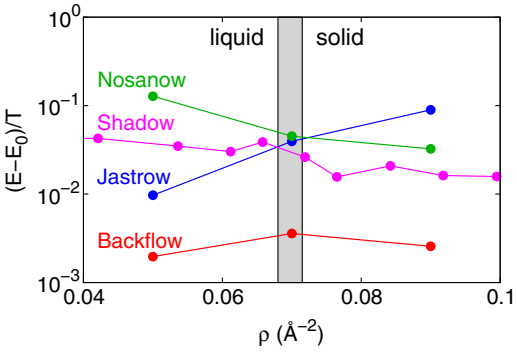

FIG. 4. Error of the ground state energy of liquid and solid ^{4}He in two dimension in units of the kinetic energy T across the liquid-solid coexistence region (shaded) [36], using various wave functions: Shadow [37], Jastrow, Nosanow, and iterative backflow network (5 iteration layers at coexistence, 4 layers otherwise).

TABLE II. Ground-state energy per particle, in K, of liquid ^{3}He in three dimensions at equilibrium and freezing densities, obtained with VMC (E_{VMC}/N) and fixed-node DMC (E_{FNDMC}/N) using different types of trial wave functions together with the experimental value from Ref. [39] (notations as in Table I). The results from entry S3BF4 of Table I of Ref. [15] are corrected by a perturbative estimate of the difference due to their use of a different [40] pair potential $v(r)$.

	$\rho = 0.01635$ Å^{-3}		
	E_{VMC}/N	σ^2/N	E_{FNDMC}/N
J	−1.6812(17)	38.23	−2.0925(16)
BF1	−2.0844(13)	16.70	−2.2760(10)
BF2	−2.2278(23)	8.10	−2.3190(14)
BF3	−2.2576(15)	5.60	−2.3288(14)
Extrapolation	−2.34(1)		
Reference [15]	−2.168(3)	14	−2.306(4)
Experiment [39]		−2.481	
	$\rho = 0.02380$ Å^{-3}		
	E_{VMC}/N	σ^2/N	E_{FNDMC}/N
J	0.7582(32)	111.06	−0.2890(43)
BF1	0.0952(17)	65.03	−0.5572(41)
BF2	−0.3661(42)	29.43	−0.6545(15)
BF3	−0.5177(32)	17.47	−0.6911(16)
BF4	−0.5531(27)	14.41	−0.7013(42)
Extrapolation	−0.723(3)		
Reference [15]	−0.127(5)	49	−0.6485(4)
Experiment [39]		−0.918	

They lie between BF1 and BF2, showing that the implicit inclusion of correlations at all orders through backflow iteration is more effective than explicit construction of successive n-order terms.

Due to the lack of exact benchmark results for this fermionic case, we compare our results to the experimental equation of state [39]. Although the improvement over previous variational and fixed-node energies remains significant, our best estimate, the extrapolation to zero variance [24], is higher than the experimental energy by 0.14 K at equilibrium density, and by 0.19 K at freezing. This discrepancy is surprising, since the error of the zero-variance extrapolation is of order of 0.01 K for ^{4}He in two and three dimension and also for small systems of ^{3}He in two dimensions [13].

In summary, we demonstrated the quality of our backflow network for quantitative description of bosonic and fermionic helium systems. The description of crystallization reported here shows that the network accurately describes spontaneous breaking of translational symmetry, and this holds true for density modulations induced by external potentials [24]. Beyond quantum liquids and solids, the present description provides a systematic way to improve calculations in the field of ultracold atomic gases and electronic structure problems [41], as well as a starting point for exploring its connection to neural network theory. The accurate description of ground-state properties further suggests their use as trial wave functions within time-dependent variational Monte Carlo calculations [42,43] to study out-of-equilibrium time evolution of many-body quantum systems in two or three dimensional, continuous space.

M. H. is grateful to Francesco Calcavecchia and Giuseppe Carleo for seminal and stimulating discussions concerning the relation of backflow and neural network wave functions and acknowledges support from the Fondation NanoSciences (Grenoble).

[1] N. Bogoliubov, J. Phys. (USSR) **11**, 23 (1947).
[2] W. L. McMillan, Phys. Rev. **138**, A442 (1965).
[3] M. Fannes, B. Nachtergaele, and R. F. Werner, Commun. Math. Phys. **144**, 443 (1992).
[4] S. R. White, Phys. Rev. Lett. **69**, 2863 (1992).
[5] U. Schollwöck, Rev. Mod. Phys. **77**, 259 (2005).
[6] U. Schollwöck, Ann. Phys. (Amsterdam) **326**, 96 (2011).
[7] R. Orús, Ann. Phys. (Amsterdam) **349**, 117 (2014).
[8] G. Carleo and M. Troyer, Science **355**, 602 (2017).
[9] H. Saito, J. Phys. Soc. Jpn. **86**, 093001 (2017).
[10] H. Saito and M. Kato, J. Phys. Soc. Jpn. **87**, 014001 (2018).
[11] Y. Nomura, A. Darmawan, Y. Yamaji, and M. Imada, Phys. Rev. B **96**, 205152 (2017).
[12] M. Ganahl, J. Rincón, and G. Vidal, Phys. Rev. Lett. **118**, 220402 (2017).
[13] M. Taddei, M. Ruggeri, S. Moroni, and M. Holzmann, Phys. Rev. B **91**, 115106 (2015).
[14] K. Schmidt, M. H. Kalos, M. A. Lee, and G. V. Chester, Phys. Rev. Lett. **45**, 573 (1980).
[15] M. Holzmann, B. Bernu, and D. M. Ceperley, Phys. Rev. B **74**, 104510 (2006).
[16] M. Foulkes, L. Mitas, R. Needs, and G. Rajagopal, Rev. Mod. Phys. **73**, 33–83 (2001).
[17] D. M. Ceperley, Rev. Mod. Phys. **67**, 279 (1995).
[18] S. Baroni and S. Moroni, Phys. Rev. Lett. **82**, 4745 (1999).
[19] A. Sarsa, K. E. Schmidt, and W. R. Magro, J. Chem. Phys. **113**, 1366 (2000).
[20] S. Vitiello, K. Runge, and M. H. Kalos, Phys. Rev. Lett. **60**, 1970 (1988).
[21] F. Pederiva, S. A. Vitiello, K. Gernoth, S. Fantoni, and L. Reatto, Phys. Rev. B **53**, 15129 (1996).
[22] F. Calcavecchia, F. Pederiva, M. H. Kalos, and T. D. Kühne, Phys. Rev. E **90**, 053304 (2014).
[23] F. Calcavecchia and M. Holzmann, Phys. Rev. E **93**, 043321 (2016).
[24] See Supplemental Material at http://link.aps.org/supplemental/10.1103/PhysRevLett.120.205302, which includes Refs. [25, 26], for more details on the network wave function, comments on the zero-variance extrapolation, pair distribution functions of 2D ^{4}He, and results for an inhomogeneous system.
[25] M. Holzmann, D. M. Ceperley, C. Pierleoni, and K. Esler, Phys. Rev. E **68**, 046707 (2003).

[26] P. López Ríos, A. Ma, N. D. Drummond, M. D. Towler, and R. J. Needs, Phys. Rev. E **74**, 066701 (2006).
[27] R. P. Feynman and M. Cohen, Phys. Rev. **102**, 1189 (1956).
[28] V. R. Pandharipande and N. Itoh, Phys. Rev. A **8**, 2564 (1973).
[29] K. E. Schmidt and V. R. Pandharipande, Phys. Rev. B **19**, 2504 (1979).
[30] R. A. Aziz, V. P. S. Nain, J. S. Carley, W. L. Taylor, and G. T. McConville, J. Chem. Phys. **70**, 4330 (1979).
[31] S. Sorella, M. Casula, and D. Rocca, J. Chem. Phys. **127**, 014105 (2007).
[32] S. Moroni, D. E. Galli, S. Fantoni, and L. Reatto, Phys. Rev. B **58**, 909 (1998).
[33] M. Rossi, M. Nava, L. Reatto, and D. E. Galli, J. Chem. Phys. **131**, 154108 (2009).
[34] R. Rota, J. Casulleras, F. Mazzanti, and J. Boronat, Phys. Rev. E **81**, 016707 (2010).
[35] L. H. Nosanow, Phys. Rev. Lett. **13**, 270 (1964).
[36] M. C. Gordillo and D. M. Ceperley, Phys. Rev. B **58**, 6447 (1998).
[37] B. Krishnamachari and G. V. Chester, Phys. Rev. B **61**, 9677 (2000).
[38] For the liquid-solid transition in 2D ^{4}He we retain only two–body terms in the network wave functions; this illustrates the robustness of our approach against the quality of the zeroth iteration.
[39] R. A. Aziz and R. K. Pathria, Phys. Rev. A **7**, 809 (1973); the energy at equilibrium density is from A. L. Reesink, Ph.D. thesis, University of Leiden, 2001.
[40] T. Korona, H. L. Williams, R. Bukowski, B. Jeziorski, and K. Szalewicz, J. Chem. Phys. **106**, 5109 (1997).
[41] S. Moroni and M. Holzmann (unpublished).
[42] G. Carleo, F. Becca, M. Schirò, and M. Fabrizio, Sci. Rep. **2**, 243 (2012).
[43] G. Carleo, L. Cevolani, L. Sanchez-Palencia, and M. Holzmann, Phys. Rev. X **7**, 031026 (2017).